Electronic Supplementary Information

Tunable nanoblock lasers and stretching sensors

T. W. Lu*, C. Wang, C. F. Hsiao and P. T. Lee*

Department of Photonics and Institute of Electro-Optical Engineering, National Chiao Tung University,
Rm. 401 CPT Building, 1001 Ta-Hsueh Road, Hsinchu 30010, Taiwan

Email: T. W. Lu (tsanwenlu@gmail.com) or P. T. Lee (potsung@mail.nctu.edu.tw)

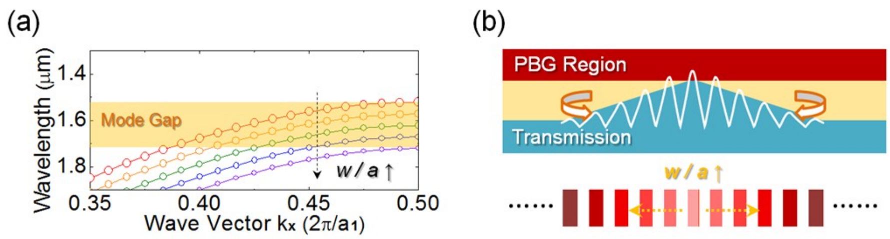

Fig. S1 (a) Plot of the dielectric band frequency under different *w/a* values. The dielectric band edge frequency (wavelength) decreases (increases) when *w/a* increases owing to the increased effective modal index. Thus, the frequency of the dielectric band propagating in the nanoblocks with small *w/a* values will lie within the partial photonic band gap (PBG, shadow region) of the dielectric band propagating in the nanoblocks with large *w/a* values. This shadow region constitutes the mode-gap effect. (b) Schematic diagram of 1D periodic nanoblocks with double hetero-interfaces formed by gradually varying *w/a*. For the allowed propagating dielectric band in the center of this structure, the double hetero-interface forms a frequency cave; in other words, the outer lattice provides confinement based on the mode-gap effect to form a nanocavity.

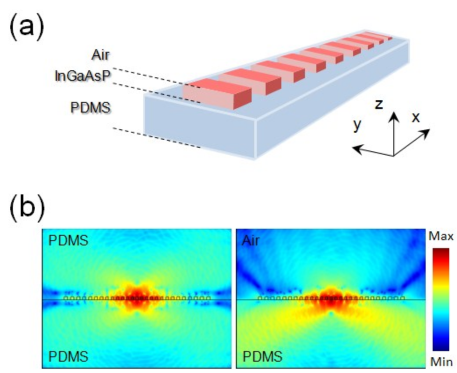

Fig. S2 (a) Schematic diagram of 1D periodic nanoblocks placed on the PDMS substrate. (b) Theoretical power flows (in log scale, along the *xz*-plane) of the confined dielectric modes in nanoblock cavities within and on the PDMS substrate. Obviously, the panel on the right shows significant radiation leaking into the PDMS substrate relative to the leakage into the top air cladding.

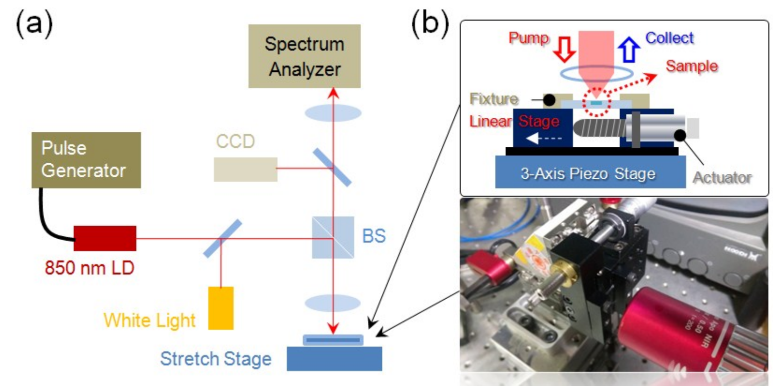

Fig. S3 (a) The excitation laser pulse with an 800 kHz repetition rate and a 15 ns pulse width is focused to a spot with a diameter of 2.5 μm via a long working distance objective lens (100×). Lasing emissions from the nanoblock lasers are collected via the same objective lens and fed into the spectrum analyzer. The sample position and stretching are controlled by a 3-axis piezo stage and the attached linear stage, respectively. (b) The schematic diagram (top) and picture (bottom) of the stretching stage in the micro-PL system. The devices are fixed on the linear stage and are stretched by the actuator.

Supplementary Note 1: Defining "stretching" in experiments

In our stretching experiments, all the PDMS films (thickness <2 mm) will be cut to a size of 2 × 1 cm^2, as shown by the inset of Fig. S4(a). Both sides of the device are then clamped along the dotted lines shown in the inset of Fig. S4(a) via the fixture of the stretching stage illustrated in Fig. S3(b), which leaves a region with a length L_{PDMS} of 1.4 cm for stretching. The elongations (in percentage) in this report is defined by the variation of L_{PDMS} and is verified by the elongation of nanoblocks under stretching. The former is directly calculated by the working distance of the actuator in the stretching stage; the latter is evaluated via the optical microscope image using pixel brightness analysis. Figure S4(b) shows the optical microscope images of the nanoblocks with elongations of 0 (A), 3.6 (B), 7.2 (C), 10.9 (D), 16.3 (E), 20.0 (F), and 23.6 % (G) by stretching, where the linear elongation can be clearly observed. Figure S4(a) shows that the elongations defined by the variation of L_{PDMS} and the nanoblocks are consistent with each other.

In addition, the contraction of the PDMS film by compressing along the*y*-direction that is due to the positive Poisson's ratio is measured by the knife-edge method. As shown by the inset of Fig. S4(c), a divergent laser spot is incident on the edge of the PDMS film and projected on the screen 1.75 m away from the PDMS. Via the displacement of the shaded edge of the projected spot, we can precisely evaluate the contraction of the PDMS film along the *y*-direction when the PDMS is stretched along the *x*-direction, as shown in Fig. S4(c). Via linear fitting, 1 % elongation by stretching along the *x*-direction will lead to a 0.33 % contraction of the PDMS film by compressing along the *y*-direction.

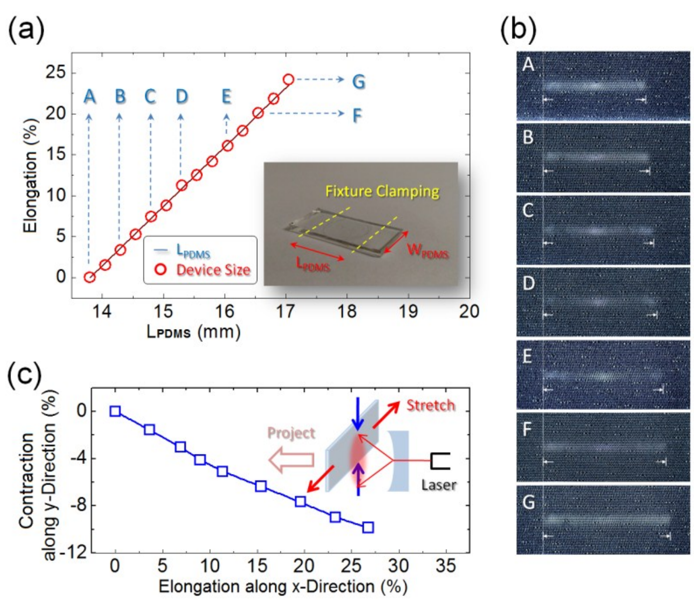

Fig. S4 (a) The elongation (in percentage) is defined by the variation of L_{PDMS} and is verified by (b) the optical microscope images of nanoblocks when the PDMS film is stretched along the *x*-direction. The inset of (a) shows the picture of the PDMS film with embedded nanoblocks. (c) Evaluated contraction along the*y*-direction via the knife-edge method upon stretching the PDMS film along the *x*-direction.

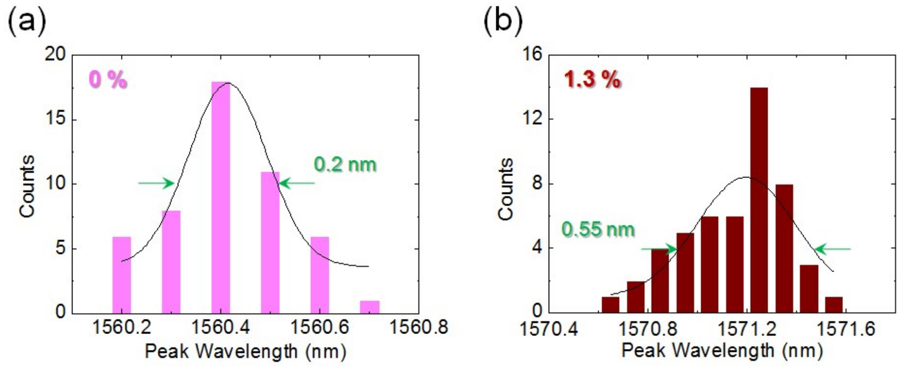

Fig. S5 Lasing wavelength statistical distribution for the device in Fig. 4(b) under (a) relaxation and (b) 1.3 % elongation during 50 cycles of relaxation and stretching. Their distribution linewidths are measured via Gaussian fitting to be 0.2 and 0.55 nm, respectively, which represent the wavelength uncertainties in the states of relaxation and stretching, respectively. These wavelength uncertainties are an important reliability index for tunable nanolasers, and determine the minimum resolution $\delta\lambda$ in the spectrum of the stretching sensors.

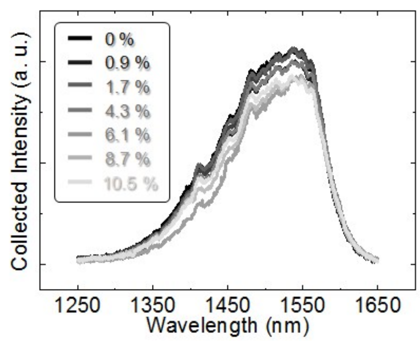

Fig. S6 The PL spectra of InGaAsP MQWs embedded within PDMS under different elongation values from 0 to 10.5 %. The PL intensity slightly degrades with stretching.

Supplementary Note 2: Evaluating index change of polydimethylsiloxane (PDMS) under stretching

According to the schematics shown in Fig. S7(a), the transmitted laser power through the PDMS film upon stretching can be expressed as follows:

$$P_{out} = P_{in}[(1-R)^2 + (1-R)^2R^2], \tag{S1}$$

$$P_{out}' = P_{in}[(1-R')^2 + (1-R')^2R'^2], \tag{S2}$$

where P_{in} represents the incident laser power. The P_{out}(P_{out}') and R (R') values represent the transmitted laser power and reflectivity of the PDMS/air interface of PDMS in a state of relaxation (stretching), respectively. The reflectivity values R and R' can be expressed as $(n_{air}-n_{PDMS})^2$ / $(n_{air} + n_{PDMS})^2$ and $(n_{air}-n_{PDMS}')^2$ / $(n_{air} + n_{PDMS}')^2$, respectively, where n_{air}, n_{PDMS}, and n_{PDMS}' represent the indices of air (set as 1), relaxed PDMS film (set as 1.405 in the near-infrared region), and stretched PDMS film, respectively. Furthermore, $(n_{PDMS}'-n_{PDMS})$ can be evaluated by measuring P_{out}' / P_{out} according to these two equations, as shown in Fig. S7(b).

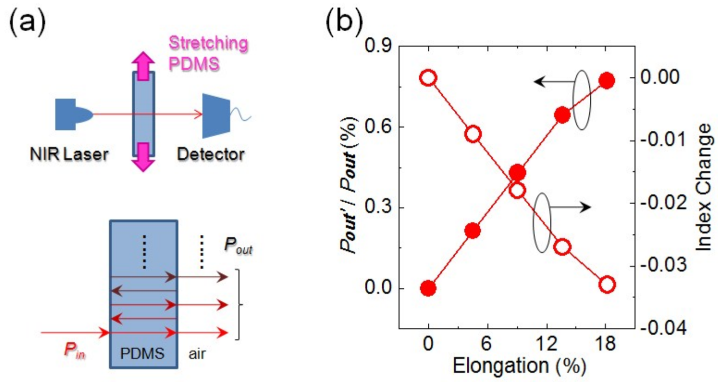

Fig. S7 (a) Schematic diagram of measurement setup for evaluating the index change of PDMS film under stretching. The index variation can be evaluated by the transmitted laser power variation of a collimated near-infrared (NIR) laser beam incident on the PDMS film before and after stretching. (b) The measured P_{out}' / P_{out} and evaluated index change when the PDMS film undergoes elongation from 0 to 18 % by stretching, where P_{out} and P_{out}' represent the transmitted laser power through the PDMS film in the states of relaxation and stretching, respectively. By substituting them into Eqs.(S1) and (S2), we can calculate the index variation for the PDMS film under 1 % elongation to be −0.002. This index reduction has been taken into consideration for all the simulations in this report.

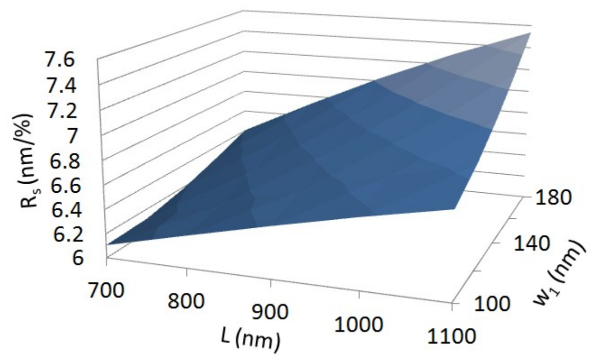

Fig. S8 Theoretical R_s values of the 3D FEM simulation for nanoblock cavities with values of w_1 = 100–180 nm and L = 700–1100 nm, with a_1 and t fixed at 340 and 220 nm, respectively. Within these ranges, R_s varied from 6.1 to 7.5 nm/%. We can see that R_s increases with w_1 and/or L; in other words, R_S monotonically increases with the resonance wavelength of the nanocavity.

Supplementary Table

	Density (kg/m³)	Poisson's Ratio	Young's Modulus (Pa)
InGaAsP	4914	0.350	6.27×10^{10}
PDMS	965	0.495	8.68×10^{5}

Table S1 Material parameters of InGaAsP and PDMS used in simulation of Fig. 4(a).